The concentration quenching of photoluminescence in Eu^{3+}-doped La$_2$O$_3$

V. Đorđević, Ž. Antić, M. G. Nikolić and M. D. Dramićanin

Vinča Institute of Nuclear Sciences, University of Belgrade,
PO Box 522, Belgrade, Serbia

Abstract

This work explores the influence of dopant concentration on photoluminescent emission and kinetics of Eu^{3+}-doped $(0.2-10\,\mathrm{at.\%})$ nanocrystalline lanthanum-oxide powders. The X-ray diffraction analysis confirmed that all samples crystallize in La$_2$O$_3$ hexagonal phase with space group P$^{\bar{3}}m1$. Transmission electron microscopy showed particles with non-uniform shape and diverse size distribution with an average particle size of $(95 \pm 5)\,\mathrm{nm}$. The room temperature photoluminescence spectra of all samples contain characteristic Eu^{3+} luminescence lines with the most pronounced red ^{5}D$_0 \rightarrow {}^7$F$_2$ emission at about $626\,\mathrm{nm}$. The maximum intensity of red emission is observed for the sample containing $5\,\mathrm{at.\%}$ of Eu^{3+} ions. The emission kinetics was recorded in the temperature range from $10\,\mathrm{K}$ to $300\,\mathrm{K}$. The maximum lifetime value of $0.98\,\mathrm{ms}$ obtained for the sample with $0.5\,\mathrm{at.\%}$ Eu^{3+} at room temperature increases up to $1.3\,\mathrm{ms}$ at $10\,\mathrm{K}$.

1. Introduction

Materials that absorb energy and subsequently emit it as ultraviolet, visible or infrared light, are called phosphors. They are usually composed of a transparent host doped with activator ions, typically a transition metal or rare-earth (RE). Due to electronic configuration and size of the lanthanide atoms rare-earth sesquioxides are well known host materials with broad transparency range, high light output and large energy band gap. [1] Similar ionic radii [2], electronic structures and electronegativity [3] of host lanthanide ions allow their easy replacement by luminescence-active REu^{3+} ions in a wide range of concentrations, without considerably defecting the lattice structure.

According to ion radius and temperature, rare earth sesquioxides can crystallize in three polymorphic forms below 2000°C: cubic (C), monoclinic (B) and hexagonal (A); from which they transform to high temperatures H- and X-forms [4]. In the series of RE trivalent ions La^{3+} has the largest diameter and La$_2$O$_3$ crystallizes in an A-type hexagonal structure with space group P$^{\bar{3}}m1$ (No. 164). Comparing to other rare-earth host materials (Lu$_2$O$_3$, Gd$_2$O$_3$, etc.) low-cost lanthanum-oxide (La$_2$O$_3$) has a number of industrial

and technological applications [5-12]. It can be an effective additive in various polymers [13-15], an important component of new advanced ceramics [16,17], or a component in specialized optical glasses [18,19]. Although there are only a few reports on preparation and luminescence of rare earth doped La_2O_3-based phosphors [20-25] its low phonon energy $\sim 400 \, cm^{-1}$, [20] makes them a potential material for up- and down-converting phosphors [20-25]. However, lanthanum-oxide based materials have to be managed with precaution due to their high sensitivity to the ambient conditions [26,27].

Due to the most pronounced red emission, europium-doped materials are commonly known as red phosphors. Europium non-degenerated ground ($^7F_0$) and excited ($^5D_0$) states, together with non-overlapping $^{2S+1}L_J$ multiplets, give emission spectra with clear dependence on host material site symmetry [28] and makes Eu^{3+} ion a well-known structural probe.

In this study, a set of Eu^{3+}-doped nanocrystalline lanthanum-oxide (La_2O_3) powders was prepared by a polymer complex solution (PCS) method [29]. Characterization of nanopowders phase, morphology and crystallinity was performed using X-ray diffraction (XRD) and transmission electron microscopy (TEM). Photoluminescent (PL) emission and kinetics measurements have been performed in the range from $10 \, K$ to $300 \, K$, using the 464-nm excitation. In order to obtain the strongest photoluminescent intensity and the longest lifetime the effect of different Eu^{3+} ion doping concentrations ($0.2 - 10 \, at.\%$) in La_2O_3 host were systematically investigated.

2. Experimental

The La_2O_3 samples doped with x at.using polymer complex solution method that we have successfully used for various rare-earth oxide systems and their solid solutions [30-34]. Water solutions of stoichiometric quantities of La and Eu-nitrate were prepared by dissolving the appropriate quantities of La_2O_3 (Alfa Aesar, 99.9%) and Eu_2O_3 (Alfa Aesar, 99.9%) in a hot nitric acid. Polyethylene glycol-PEG 200 (Alfa Aesar, $\bar{M}_W = 200$) was added to the solutions in a 1:1 mass ratio to the sum of used oxides. After forming the metal-PEG solution and stirring at 80°C, solid complex was formed and subsequently combusted at 800°C in the air, and calcinated at the same temperature for 2 hours. The resulting white powders were immediately characterized, having in mind their high affinity to react with atmospheric water [35].

The X-ray diffraction measurements were performed using a Philips PW 1050 instrument, with Ni filtered Cu $K_{\alpha1,2}$ radiations. Diffraction data were recorded in a 2θ range from $10°$ to $90°$ counting for $3 \, s$ in $0.05°$ steps. Microstructural characterization was done using a FEI Tecnai G2 30F transmission electron microscope operating at $300 \, kV$ and equipped with a Schottky field emission source (STEM). Prior to applying the sample on a copper-carbon grid, the powder was crushed in an agate mortar and then sonicated in ethyl alcohol. The photoluminescence (PL) measurements were performed over a temperature range $10 - 300 \, K$ on a Horiba Jobin-Yvon Model FHR1000 spectrofluorometer system, utilizing as an excitation source the optical parametric oscillator (OPO) EXPLA NT342. An ICCD Jobin-Yvon 3771 detector was used both for emission spectra and

lifetime measurements, while the temperature was controlled with a closed-cycle cryostat (Advanced Research System DE202-AE) equipped with a Lakeshore model 331 controller. All PL experiments were done on the pellets prepared by compacting the powders under a load of 5 tonnes, without any additives.

3. Results and discussion

The X-ray diffraction analysis revealed that all samples crystallize in La_2O_3 hexagonal phase with space group $P\bar{3}m1$ (No. 164). The XRD pattern of representative La_2O_3:5 at.% Eu^{3+} sample is presented in Fig. 1. The main diffraction peaks are indexed according to the PDF-05-0602 (La_2O_3). No other phases or impurities were detected in the diffractogram indicating that Eu3+ ions have been effectively incorporated into the La_2O_3 host lattice. Due to the smaller ionic radius of Eu^{3+} ion ($= 0.947$ Å) compared to the La^{3+} ion ($= 1.032$ Å) [36], a small shift of the diffraction peaks toward higher angles confirmed the europium incorporation in the host material. Crystal coherence size of around 5.7 nm was calculated by the Debay-Sherrer formulae using FWHM of (101) reflection.
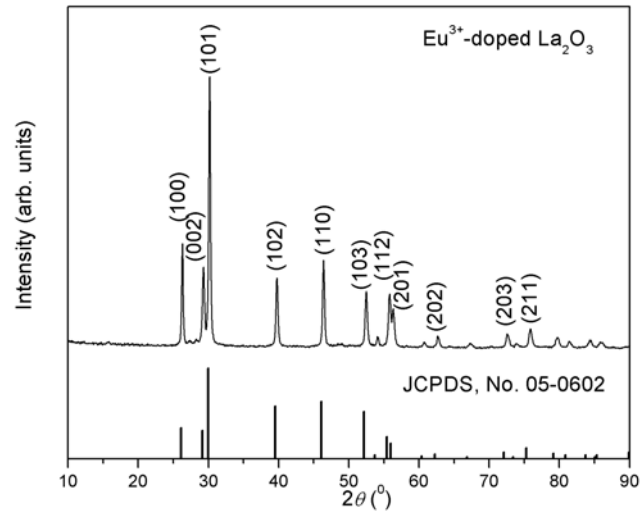

Figure 1. XRD pattern of Eu^{3+}- doped La_2O_3 powder sample. The diffraction peaks are indexed according to the PDF-050602 (La_2O_3).

A representative TEM image of La_2O_3:5 at.% Eu^{3+} sample presented in Fig. 2a shows the particles with non-uniform shape and a diverse size distribution. The TEM images were used for the average particle size analysis taking into account about 200 particles and the obtained size distribution is presented in Fig. 2b. Due to the fact that the particles have irregular shapes the largest axis of the particles were recorded and reported in the histogram. The average size is found to be (95 ± 5) nm. From the STEM image in Fig. 2c, two particles have been selected for the X-ray microanalysis. The X-ray emission spectra (Fig. 2d) confirmed the presence of all constituent atoms including Eu dopant in the particles.
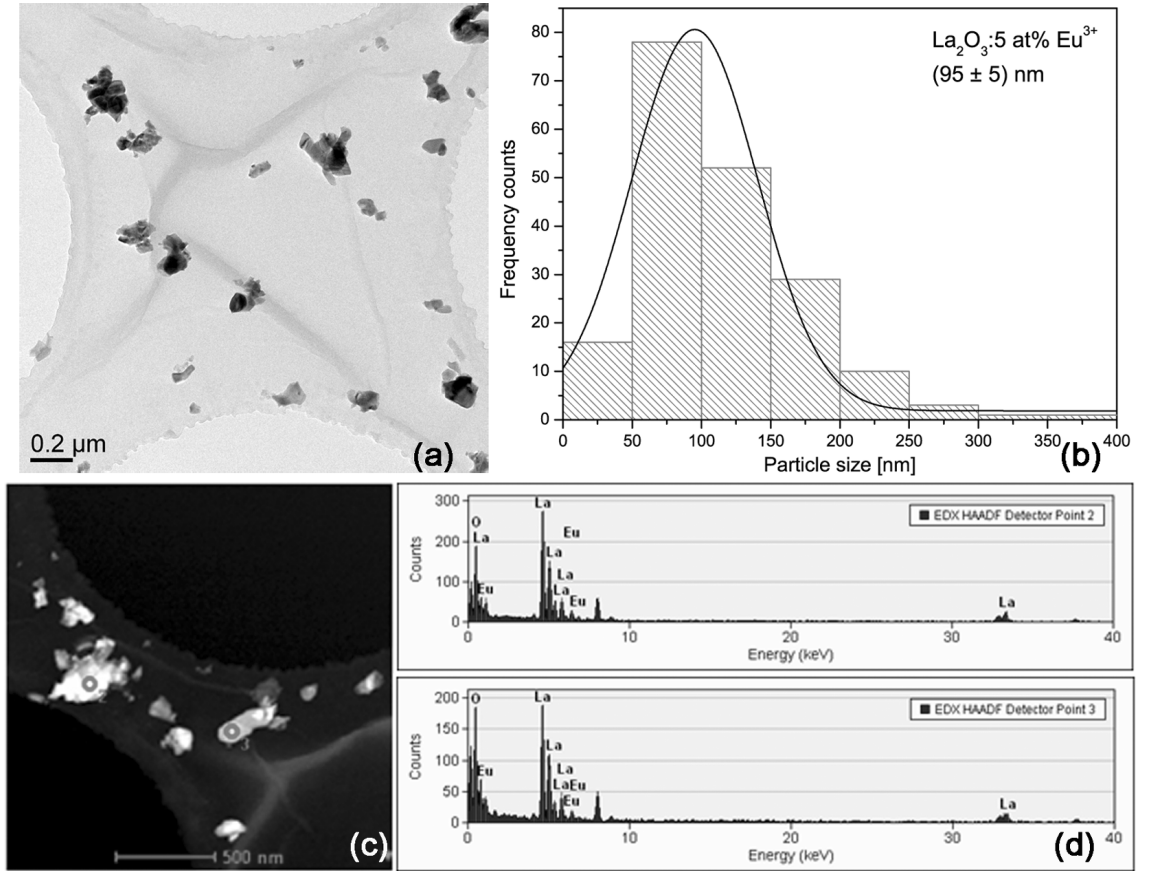
Figure 2. Microstructural characterization of La_2O_3:5 at.% Eu^{3+}: (a) Bright Field TEM image, (b) respective size distribution of the particles, (c) STEM image of the studied sample with particles having a bright contrast, (d) X-Ray emission spectra collected from two different particles. The histogram shown in Fig.2b was fitted by a Gaussian distribution curve.

The photoluminescence spectra of samples with different Eu^{3+}-dopant concentrations, recorded at room temperature, are presented in Fig. 3. Five characteristic bands associated to $^5D_0 \rightarrow {}^7F_J$ ($J = 0, 1, 2, 3, 4$) Eu^{3+} spin forbidden $f - f$ transitions, are clearly visible. Imposed by non-centrosymmetric C_{3v} point group symmetry of the crystal field around Eu^{3+} ion in La_2O_3, $^5D_0 \rightarrow {}^7F_0$ transition line is markedly visible and typical red $^5D_0 \rightarrow {}^7F_2$ transition line is dominant. An increase in the luminescent centre concentration should be accompanied by an increase in the emitted light intensity due to higher absorption efficiency. However, above a certain concentration, the luminescence intensity starts to decrease due to the concentration quenching of luminescence. The quenching starts when there is a sufficient reduction in the average distance between luminescent centres to favor nonradiative energy transfer [37]. The emission intensity of europium $^5D_0 \rightarrow {}^7F_2$ transition with the maximum located at 626 nm as a function of Eu^{3+}-dopant concentration is shown as inset in Fig. 3. As it can be clearly seen, the red emission increases from

0.2 at.% reaching maximum at 5 at.%, and decreases again for higher concentrations of Eu^{3+}-dopant.

Temperature dependence of emission spectra of the sample with the highest intensity (La_2O_3:5 at.% Eu) was previously studied [30]. There was no significant difference in the emission intensities of europium $^5D_0 \rightarrow {}^7F_J$ ($J = 0, 1, 2, 3, 4$) transitions due to low phonon energy of the La_2O_3 host matrix.

Decay times of the $^5D_0$- level in all Eu^{3+}-doped La_2O_3 samples are recorded at 626 nm under 464 nm excitation. All decay profiles are nearly exponential and could be fitted with a single exponential function showing that only one deexcitation process is present. The obtained lifetime values as a function of Eu3+ concentration are presented in Fig. 4a. The lifetime values are about the same up to 3 at.% with maximum at 0.5 at.% and decrease sharply for higher concentrations of the Eu^{3+}-dopant. The trend indicates that the resonant energy transfer between two identical Eu^{3+} canters is least prominent for the La_2O_3:0.5 at% Eu^{3+} sample. For that reason the La_2O_3:0.5 at% Eu^{3+} sample was characterized in the temperature range from 10 K to 300 K, as presented in Fig. 4b. The lifetime values decrease from 1.3 ms at 10 K to 0.98 ms at 300 K. Since the decay time of the $^5D_0$- level in the Eu^{3+}-doped matrices is a strong indicator of the transfer of nonradiative energy throughout the material, the higher the lifetime is the nonradiative deexcitation is less competitive to the radiative one. The lifetime temperature dependence in the sample is a consequence of phonon statistics and increased multi-phonon relaxation at higher temperatures that lead to faster emission quenching.
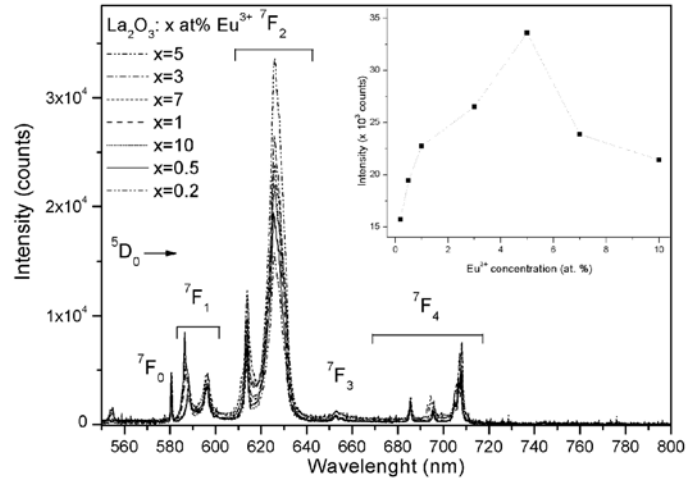

Figure 3. Emission spectra of La_2O_3:x at.% Eu^{3+} (x = 0.2; 0.5; 1; 3; 5; 7; 10) with dependence of the red emission intensity (transition at 626 nm) vs. Eu^{3+} concentration as inset.
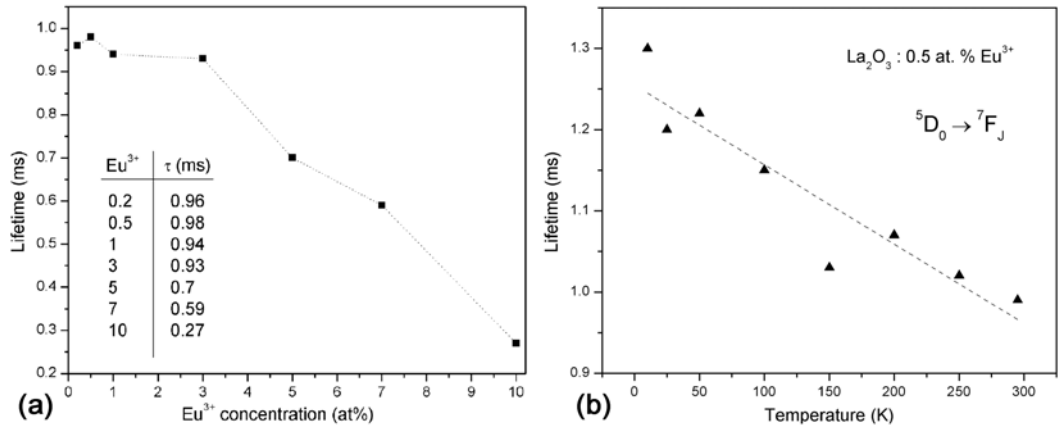
Figure 4. (a) The change of $^5D_0$ level lifetime with Eu^{3+} doping concentration for La_2O_3: x at.% Eu^{3+} (x = 0.2; 0.5; 1; 3; 5; 7; 10) samples and (b) Temperature dependence of lifetime of $^5D_0$ emission in the La_2O_3: 0.5 at% Eu^{3+} sample.

4. Conclussion

The Eu^{3+}-doped La_2O_3 samples, produced via the polymer complex solution synthesis were studied in order to study the influence of dopant concentration on the photoluminescent emission and kinetics. Regardless of different dopant concentrations, all samples crystallize in a hexagonal phase. The STEM analysis confirmed successful europium doping of La2O3 samples. The maximum photoluminescence emission intensity is observed for 5 at.% Eu^{3+}-doped La_2O_3 sample. The maximum lifetime value was found for the 0.5 at.% Eu^{3+}-doped sample and it decreased significantly after 3 at.% Eu^{3+}. The summarized results indicate that the optimal dopant concentration of Eu^{3+} ion in La_2O_3 host could be 3 at.%, since for that concentration both emission and kinetic characteristics are significantly high.

Acknowledgments

References

[1] G. Adachi, N. Imanaka, Z. Kang, *Binary Rare Earth Oxides*, (Kluwer Academic Publishers, Amsterdam, 2004).

[2] R. D. Shannon, Acta Crystallogr. Sect. A **32**, 751 (1976).

[3] D. R. Lide, *CRC Handbook of Chemistry and Physics*, 87th edition, pp. 9-77, (CRC Press, 2006).

[4] G. Adachi and N. Imanaka, Chem. Rev. **98**, 1479 (1998).

[5] T. Tanabe, Y. Nagai, K. Dohmae, N. Takagi, N. Takahashi, S. Matsumoto, H. Shinjoh, Operando, Appl. Catal. B **105**, 41 (2011).

[6] S. Sato, R. Takahashi, M. Kobune, H. Inoue, Y. Izawa, H. Ohno, K. Takahashi, Appl. Catal. A **356**, 64 (2009).

[7] K. Sutthiumporn, S. Kawi, Int. J. Hydrogen Energy **36**, 14435 (2011).

[8] K. Tanaka, Y. Sekine, K. Oshima, Y. Tanaka, M. Matsukata, E. Kikuchi, Chem. Lett. **41**, 351 (2012).

[9] B. Sen, H. Wong, J. Molina, H. Iwai, J.A. Ng, K. Kakushima, C.K. Sarkar, Solid-State Electron. **51**, 475 (2007).

[10] S. S. Kale, K. R. Jadhav, P. S. Patil, T. P. Gujar, C. D. Lokhande, Mater. Lett. **59**, 3007 (2005).

[11] L. Zhang, Z. Sun, F. Yu, H. Chen, Bioinorg. Chem. Appl. **2011**, 853048 (2011).

[12] M. Leskelä, K. Kukli, M. Ritala, J. Alloys Compd. **418**, 27 (2006).

[13] Y. Li, B. Li, J. Dai, H. Jia, S. Gao, Polym. Degrad. Stab. **93**, 9 (2008).

[14] J. Song, C. Lu, D. Xu, Y. Ni, Y. Liu, Z. Xu, J. Liu, Polym. Int. **59**, 954 (2010).

[15] C. Feng, Y. Zhang, S. Liu, Z. Chi, J. Xu, Polym. Degrad. Stab. **97**, 707 (2012).

[16] X. Chou, J. Zhai, X. Yao, Mater. Chem. Phys. **109**, 125 (2008).

[17] O. Fabrichnaya, G. Savinykh, G. Schreiber, M. Dopita, H.J. Seifert, J. Alloys Compd. **493**, 263 (2010).

[18] T. Hiroaki, *Optical glass, optical element and optical device*, JP2009263141 (A), (November 12, 2009).

[19] M. Dyadenko, I. Levitskii, Glass Ceram. **65**, 310 (2008).

[20] S. K. Singh, A. K. Singh, D. Kumar, O. Prakash, S. B. Rai, Appl. Phys. B **98**, 173 (2010).

[21] X. Zhang, P. Yang, D. Wang, J. Xu, C. Li, S. Gai, J. Lin, Cryst. Growth Des. **12**, 306 (2012).

[22] M. Méndez, Y. Cesteros, L.F. Marsal, A. Giguére, D. Drouin, P. Salagre, P. Formentín, J. Pallarés, M. Aguiló, F. Díaz, J.J. Carvajal, Inorg. Chem. **51**, 6139 (2012).

[23] M. Nazarov, J.H. Kang, D.Y. Jeon, S. Bukesov, T. Akmaeva, Opt. Mater. **27**, 1587 (2005).

[24] J. Liu, X. Fei, X. Yu, Z. Tao, L. Yang, S. Yang, J. Non-Cryst. Solids **353**, 4697 (2007).

[25] H. Liu, L. Wang, S. Chen, B. Zou, J. Lumin. **126**, 459 (2007).

[26] P. Fleming, R.A. Farrell, J.D. Holmes, M.A. Morris, J. Am. Ceram. Soc. **93**, 1187 (2010).

[27] Y. Long, J. Yang, X. Li, W. Huang, Y. Tang, Y. Zhang, J. Rare Earths **30**, 48 (2012).

[28] K. Binnemans, C. Goller-Walrand, J. Rare Earths **14**, 173 (1996).

[29] M. Kakihana, M. Yoshimura, Bull. Chem. Soc. Jpn. **72**, 1427 (1999).

[30] R. Krsmanović, Ž. Antić, B. Bártová, M. D. Dramićanin, J. Alloys Compd. **505**, 224 (2010).

[31] R. Krsmanović, Ž. Antić, M. G. Nikolić, M. Mitrić, M. D. Dramićanin, Ceram. Int **37**, 525 (2011).

[32] V. Đorđević, M.G. Nikolić, Ž. Antić, M. Mitrić, M. D. Dramićanin, Acta Phys. Pol. A **120**, 303 (2011).

[33] Ž. Antić, R. M. Krsmanović, M. G. Nikolić, V. Đorđević, M. D. Dramićanin, Int. J. Mater. Res. **104**, 216 (2013).

[34] R. Krsmanović, Ž. Antić, I. Zeković, B. Bártová, M. D. Dramićanin, Radiat. Meas. **45**, 438 (2010).

[35] V. Đorđević, Ž. Antić, M. G. Nikolić, M. D. Dramićanin, J. Phys. Chem. Solids **75**, 276 (2014).

[36] R. D. Shannon, Acta Crystallogr. A **32**, 751 (1976).

[37] J. Solé, L. Bausá, D. Jaque, *An Introduction to the Optical Spectroscopy of Inorganic Solids*, (John Wiley & Sons, England, 2005).